

Compact, low power consumption methane sensor based on a novel miniature multipass gas cell and a CW, room temperature interband cascade laser emitting at 3.3 μm

^{1,2}Lei Dong, ¹Chunguang Li, ³Nancy P. Sanchez, ¹Aleksander K. Gluszek, ³Robert J. Griffin and ¹Frank K. Tittel

¹ Department of Electrical and Computer Engineering, Rice University, Houston, Texas 77005, USA

² State Key Laboratory of Quantum Optics and Quantum Optics Devices, Institute of Laser Spectroscopy, Shanxi University, Taiyuan 030006, China

³ Department of Civil and Environmental Engineering, Rice University, 6100 main Street, Houston, TX 77005, USA

A tunable diode laser absorption spectroscopy (TDLAS)-based methane sensor, employing a miniature dense-pattern multi-pass gas cell (MPGC) and a continuous wave, room temperature interband cascade laser (ICL), is reported. The optical integration based on an advanced folded optical path design and an efficient ICL control system with appropriate electrical power management results in a methane sensor with a small footprint ($32 \times 20 \times 17 \text{ cm}^3$) and low-power consumption (6W). The direct absorption measurement strategy allows absolute quantitative assessments without any calibration. Polynomial and least-squares fit algorithms are employed to remove the baseline of the spectral scan and retrieve CH_4 concentrations, respectively. An Allan-Werle deviation analysis shows that the measurement precision can reach 1.4 ppb for a 60 s averaging time. Continuous measurements lasting seven days were performed to demonstrate the stability and robustness of the reported methane sensor.

Keywords: laser absorption spectroscopy, methane detection, interband cascade laser, multi-pass gas cell

INTRODUCTION

The ability to monitor methane in urban or rural areas is critical,^{1,2} as methane is a key contributor to the greenhouse effect and a safety hazard in several industries, including natural gas storage, transportation, coal mining, and the handling of liquefied methane. Optical methods based on infrared laser spectroscopy are desirable for methane sensing³⁻⁷ because they do not require pretreatment and accumulation of the concentration of the analyzed sample, unlike, for example, more conventional methods such as a mass spectrometry or gas chromatography. In addition, optical methods provide high precision remote sensing capabilities and fast response.

Tunable diode laser absorption spectroscopy (TDLAS) is an increasingly important optical method for trace gas detection;⁸⁻¹¹ In TDLAS either a near or mid-IR semiconductor laser source is critical. Trace gas species can be detected selectively in real time with sensitivities as low as the ppb concentration level, using single mode semiconductor lasers, which can be tuned rapidly by varying the applied current. The fundamental ν_3 band of methane is located at $\sim 3.2 \mu\text{m}$. Therefore, the absorption line transitions in this spectral region are suited for sensitive CH_4 trace gas detection. Single mode, room temperature laser sources emitting continuous-wave (CW) in the $3\text{--}4 \mu\text{m}$ range with reasonable output and electrical power consumption became recently commercially available. Commercially obtainable quantum cascade lasers (QCLs) are limited to wavelengths above $4 \mu\text{m}$.¹² In 2009, a gallium antimonide (GaSb)-based interband cascade laser (ICL) design initiated a new pathway for mid-IR sensing.¹³⁻¹⁵ Laser diodes based on such a design provide CW radiation between $3.0 \mu\text{m}$ and $4.0 \mu\text{m}$ at room temperature. ICLs are compact, and an intrinsic distributed feedback (DFB) structure permits CW tuning with spectral linewidths of $< 10 \text{ MHz}$.

The other key component in TDLAS is the multipass gas cell (MPGC), which provides a long absorption path length for trace gas sensing, because the measurement sensitivity is improved by increasing the effective optical path length.¹⁶ For example, conventional White and Herriott gas cells¹⁷⁻¹⁸ with absorption path lengths on the order of 10 m have typical physical lengths of $\sim 30 \text{ cm}$ and volumes of 250 mL for a Herriott cell and 2 L for a White cell, which is an unsatisfactory match for the compact ICL size. This mismatch in sizes was addressed by Sentinel Photonics/Aeris Technologies by means of the design and development of an ultra-compact MPGC consisting of two inexpensive standard concave spherical mirrors using a novel, dense spot pattern, which is more complex than the typical traditional circular or elliptical beam patterns.¹⁹⁻²¹ Such a novel MPGC design offers a 54.6-m optical path length in a physical size of $17 \times 6.5 \times 5.5 \text{ cm}^3$ with a 220-mL sampling volume and thereby obtains a sensor platform that is more than 10 times smaller than conventional designs with equivalent sensitivity. In this paper, we report the development of a compact, low power consumption methane sensor system using the combination of two recent novel techniques: a compact ICL and a small MPGC.

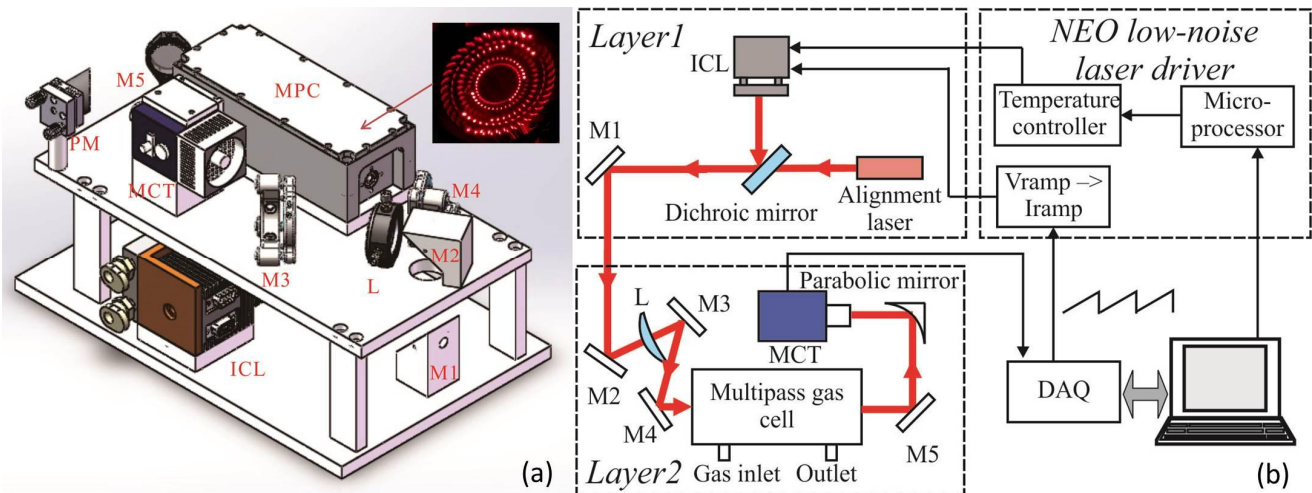


FIG. 1. (a) Photo-rendered CAD image of the optical methane sensor core showing the compact optical integration with dimensions of length (32 cm), width (20 cm) and height (17 cm). Inserted image: dense spot pattern of the ultra-compact multi-pass gas cell. (b) Schematic of a compact, calibration-free, low power methane sensor. ICL: interband cascade laser; M: plane mirror; L: lens; PM: parabolic mirror; MPC: Multi-pass gas cell; MCT: mercury-cadmium-telluride detector.

A 3D CAD model of the optical core of the methane sensor discussed is shown in Fig. 1 (a). Its schematic and final configuration are depicted in Fig. 1 (b). A Nanoplus GmbH, CW, DFB ICL mounted in a TO66 header emitting single-mode radiation at a center wavelength of 3291 nm was employed as the light source. The TO66 header was enclosed in a

5×5×5 cm³ cubic heat sink with a thermoelectric cooler (TEC). To further assist heat dissipation, a custom made copper heat exchanger was attached to the cubic heat sink, which allows the sensor platform to be connected to a compact water chiller (Solid State Cooling system, Oasis 160). The chiller is incorporated into the sensor system when it is operated in harsh environments, for example, at high ambient temperatures (>40°C). In most cases the water chiller is not used, and the ICL was operated in a temperature range between 25°C and 35°C. The ICL output power is 1.5 mW, requiring a 42 mA drive current. The current and temperature tuning coefficients of the ICL were measured -0.232 cm⁻¹/mA and -0.240 cm⁻¹/°C, respectively.

A three dimensional folded optical path design was adopted in order to minimize the CH₄ sensor system size. The methane sensor design consists of two layers, as shown in Fig. 1. The ICL, an alignment laser, and a dichroic mirror were mounted on the bottom layer (*Layer 1*). A compact alignment laser emitting visible radiation at 630 nm, was used as a guide beam for the invisible mid-infrared (mid-IR) ICL beam. The two laser beams, visible and mid-IR, were combined by means of a dichroic mirror (ISO optics, model BSP-DI-25-3). A 45-degree-angle plane mirror (M1) with respect to the horizontal plane directed the combined beams from the bottom layer (*Layer 1*) to the top layer (*Layer 2*). A second plane mirror (M2) converted the combined laser beams from the vertical to the horizontal direction. The top layer (*Layer 2*) also includes the MPGC, the mid-IR detector, and five auxiliary optical components (six mirrors and a lens). The co-propagating beams were coupled into the MPGC using a mode matching lens of 200-mm focal length (L). Two plane mirrors (M3 and M4) fold the necessary optical path into a reduced space as the focal point of the lens must be positioned at the MPGC entry aperture. The enclosure of the MPGC was made of super invar with a typical mean coefficient of thermal expansion of 10⁻⁶/°C. The dense spot pattern of the MPC obtained with the 630 nm alignment laser is shown in the insert in Fig. 1(a). An effective optical path length of 54.6 m was obtained after 435 beam passes in the MPC. The exiting, collimated ICL beam from the MPGC was subsequently focused onto a TEC, mercury-cadmium-telluride (MCT) detector (Vigo, PVI-4TE-4) using first a plane mirror (M5) and then a 35-mm focal length parabolic mirror. Stainless steel dowel pins were applied as supports between the top and bottom layers to ensure stability of the two layers of the sensor system assembly.

Selection of the optimum target absorption line is a key factor, which determines the size, cost and complexity of the sensor system. A single CH₄ line, $\nu_3R(1)$, which is located at 3038.5 cm⁻¹ and is free from the interference of other atmospheric gases (e.g., H₂O and CO₂) was selected as the target line to determine CH₄ concentration levels. This CH₄ absorption line has a line intensity of 8.958×10⁻²⁰ cm/molecule. Furthermore, this selected line allows operation of the sensor at atmospheric pressure, avoiding the use of a vacuum pump.

A compact, low-noise laser driver developed by NEO Monitors, SA (Norway) was employed to operate the ICL as shown in Fig. 1 (b). The laser driver has a size of 10 cm × 8 cm with a low noise current characteristic of ≤1 nA/√Hz and an on-board TEC driver (±3 A, 15 V). The TEC driver was programmed to control automatically the ICL temperature to 30 °C. Potential use of the methane sensor for field studies involving mobile-mode sampling requires effective and reliable electrical power management of the different components in the sensor system. The maximum TEC current and voltage determines the TEC power consumption of 5.3 W. A 12-V power supply was used because this voltage is compatible with car batteries. With a maximum laser current of 50 mA, the ICL requires 0.6-W power. Hence the total power consumption for the sensor system is ~6 W. A laptop equipped with a NI DAQ card (NI 6062E) was used to generate the 500 Hz sawtooth wave with an offset of 2.1 V and a peak-peak amplitude of 0.4 V, which was sent to the ramp input of the ICL driver, resulting in an ICL current scan from 38.3 mA to 46.1 mA. This current range corresponds to a wavelength range from 3038.04 cm⁻¹ to 3039.03 cm⁻¹. Furthermore, the laptop synchronously acquires the spectral data from the MTC detector with a sampling rate of 250 k/s.

A typical CH₄ spectrum of laboratory air is depicted in Fig. 2 together with a transmission signal from a 2.54-cm long germanium etalon with a free spectral range of 1.44 GHz. The acquired methane spectrum was processed using a four-step algorithm. In the first step, 150 methane spectra were averaged, and the absorption peak is removed from the averaged spectra. In the second step, the baseline of the spectral scan was fitted and eliminated using a fifth order polynomial as shown in Fig. 2 (dashed line). In the third step, the resulting spectrum is linearized using the quadratic polynomial obtained from the Ge etalon fringe spacing. Finally, a Lorentzian line shape was fitted to the absorption peak using a Levenberg-Marquardt least-squares fit procedure. A three-threaded program compiled by Labview executed the ramp signal output, the signal acquisition, and the digital signal processing in parallel via the NI DAQ card. Because the concentration retrieval algorithm is based on the Beer-Lambert law, it is possible to provide an absolute quantitative assessment without any calibration. The electronic system bandwidth of 300 kHz is determined by the preamplifier of the MCT detector. Spectral averaging resulted in an effective bandwidth of 2 kHz. The resulting output rate of the methane sensor is 1 Hz with a 30 % duty cycle (data acquisition time of a 300 ms/measurement time 1000 ms).

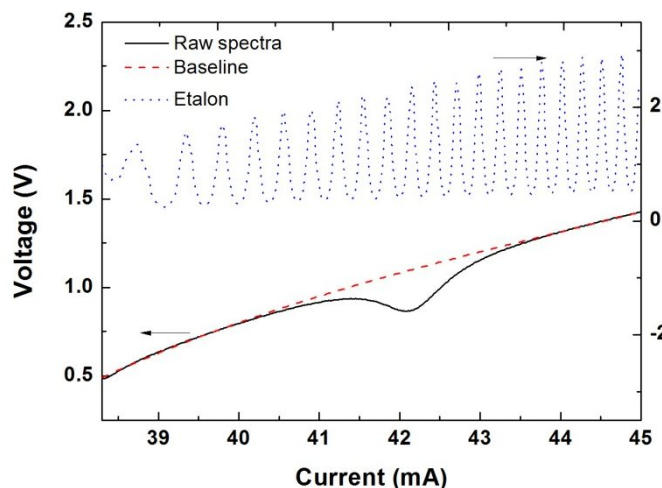


FIG. 2. Interference-free absorption line of CH_4 at 3038.5 cm^{-1} obtained from laboratory air at atmospheric pressure together with a fitted baseline and a transmission signal from a germanium etalon.

To assess the long-term stability of the CH_4 sensor system, an Allan-Werle deviation analysis was implemented based on continuous measurements of a certified 2 ppm $\text{CH}_4:\text{N}_2$ mixture (Coastal specialty gas, accuracy $\pm 5\%$) in time periods lasting ~ 1.5 hours, as shown in Fig. 3. This indicates that the 1-s measurement precision is $\sigma = 10.53 \text{ ppb}$. The Allan-Werle plot shows an optimum integration time of $\sim 60 \text{ s}$, corresponding to a precision of $\sim 1.43 \text{ ppb}$. The dashed line, proportional to $1/\sqrt{t}$, depicts the theoretically expected behavior of a system within the white noise dominated region. The Allan-Werle deviation of the reported sensor follows the $1/\sqrt{t}$ dependence for $> 60 \text{ s}$, after which time system drifts start to dominate.

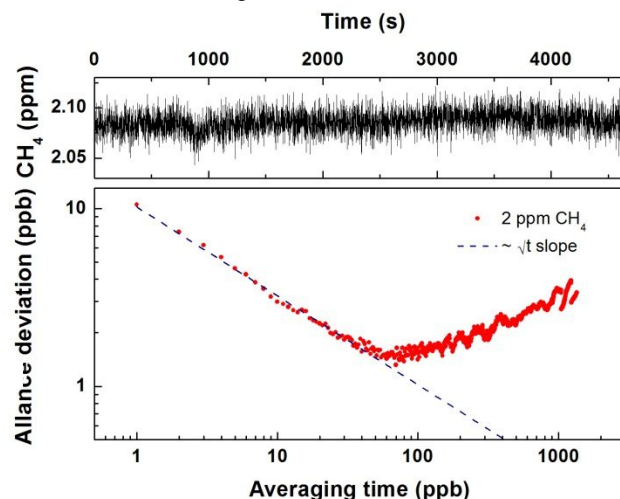


Fig.3 Allan-Werle deviation plot acquired from measurements using a certified 2 ppm CH_4 cylinder with a 1Hz sampling rate under laboratory conditions.

The developed CH_4 sensor system was located in the Space Science and Technology building on the Rice University campus. A small pump was used to sample air from outdoors. Due to the pressure gradient, the inside pressure of the MPGC is 700 Torr. The CH_4 mixing ratios measured for seven days of continuous monitoring (May 1 to May 8, 2015) are shown in Fig. 4 (a). The average CH_4 concentration was $1.96 \pm 0.1 \text{ ppm}$, with maximum and minimum concentrations of 2.7 and 1.8 ppm, respectively. From Fig. 4 (a) it is apparent, that higher CH_4 levels occur during the weekend (May 2 and 3, 2015) relative to weekdays (May 4-May 8, 2015). Longer sampling would be required to determine if weekend-weekday differences are statistically significant. The diurnal profile of CH_4 concentration (Fig. 4 (b)) shows an increase in methane concentration during the early morning, with a subsequent gradual decrease after $\sim 8:00 \text{ CDT}$ to its typical background

level of ~ 1.87 ppm. The early morning peak and the diurnal trends observed in CH_4 mixing ratios during the sampling period are in agreement with previous research work reported¹

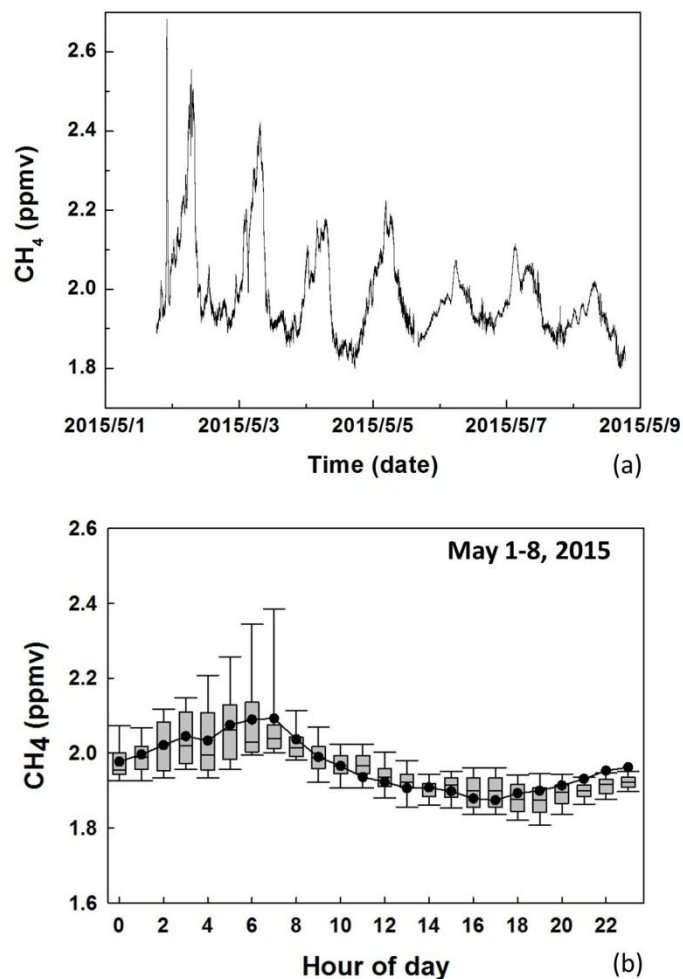


FIG. 4. (a) CH_4 concentrations measured over a 7 day period in ambient air on the Rice University campus. (b) Diurnal variations of CH_4 mixing ratios. Bottom whisker, bottom box line, top box line and top whisker indicate the 5th, 25th, 75th and 95th percentile, respectively. Line inside the boxes and continuous solid line represent the hourly median and mean of the data respectively.

Conclusions

A TDLAS based CH_4 sensor, employing a small MPGC with a $>50\text{m}$ optical path length and a CW, DFB ICL capable of room temperature operation was developed. A three dimensional folded optical path design and good electrical power management resulted in a CH_4 sensor system with a small footprint ($32 \times 20 \times 17 \text{ cm}^3$) and low electrical power consumption (6W). A polynomial fit method was employed to remove the baseline of the spectral scan, which simplifies data processing and improves the duty cycle of the data acquisition. Our results show that the measurement precision of the sensor is 10.5 ppb for a 1-s averaging time. With a 60-s averaging time, the minimum CH_4 detection can be improved to 1.4 ppbv. Deployment of the sensor system in a vehicle and mobile-mode operation tests to evaluate its performance for atmospheric CH_4 monitoring will be performed in the near future.

ACKNOWLEDGMENTS

Frank Tittel acknowledges support by the Robert Welch Foundation (Grant C-0586). Frank Tittel, Nancy Sanchez, and Robert Griffin acknowledge support by the National Science Foundation (NSF) ERC MIRTHE award and the. Lei Dong acknowledges support by National Natural Science Foundation of China (Grant #s. 61575113, 61275213), the Shanxi Natural Science Foundation (2013021004-1), and the Shanxi Scholarship Council of China (2013-011, 2013-01).

REFERENCES

- [1] I. Bamberger, J. Stieger, N. Buchmann, and W. Eugster, "Spatial variability of methane: Attributing atmospheric concentrations to emissions," *Environ. Pollut.* 190, 65-74 (2014).
- [2] F.A. Smith, S. Elliott, D.R. Blake, and F. Sherwood Rowland, "Spatiotemporal variation of methane and other trace hydrocarbon concentrations in the Valley of Mexico," *Environ. Sci. Policy* 5, 449-461 (2002).
- [3] D.G. Lancaster, R. Weidner, D. Richter, F. K. Tittel, and J. Limpert, "Compact CH₄ sensor based on difference frequency mixing of diode lasers in quasi-phases-matched LiNbO₃" *Opt. Comm.* 175, 461-468 (2000).
- [4] D.G. Lancaster and J. M. Dawes, "Methane detection with a narrow-band source at 3.4 μ m based on a Nd:YAG pump laser and a combination of stimulated Raman scattering and difference frequency mixing" *Appl. Opt.* 35, 4041-4045 (1996).
- [5] C. Fischer and M. W. Sigrist, "Trace-gas sensing in the 3.3 μ m region using a diode-based different-frequency laser photoacoustic system" *Appl. Phys. B* 75, 305-310 (2002).
- [6] D. Richter, D. G. Lancaster, R. F. Curl, W. Neu, and F. K. Tittel, "Compact mid-infrared trace gas sensor based on different-frequency generation of two diode lasers in periodically poled LiNbO₃", *Appl. Phys. B* 67, 347-350 (1998).
- [7] K. P. Petrov, S. Waltman, E. J. Dlugokencky, M. Arbore, M. M. Fejer, F. K. Tittel, L. W. Hollberg, "Precise measurement of methane in air using diode-pumped 3.4 μ m different-frequency generation in PPLN" *Appl. Phys. B* 64, 567-572 (1997)
- [8] H.I. Schiff, G.I. Mackay, and J. Bechara, "The use of tunable diode laser absorption spectroscopy for atmospheric measurements," *Res. Chem. Intermed.* 20, 525-556 (1994).
- [9] K. Krzempek, R. Lewicki, L. Nöhle, M. Fischer, J. Koeth, S. Belahsene, Y. Rouillard, L. Worschech, and F. K. Tittel, "Continuous wave, distributed feedback diode laser based sensor for trace-gas detection of ethane," *Appl. Phys. B* 106, 251-255 (2012).
- [10] M. Köhring, S. Huang, M. Jahjah, W. Jiang, W. Ren, U. Willer, C. Caneba, L. Yang, D. Nagrath, W. Schade, and F. K. Tittel, "QCL-based TDLAS sensor for detection of NO toward emission measurements from ovarian cancer cells," *Appl. Phys. B* 117, 445-451 (2014).
- [11] W. Ren, L. Luo, and F. K. Tittel, "Sensitive detection of formaldehyde using an interband cascade laser near 3.6 μ m," *Sens. Actuators B: Chem.* 221, 1062-1068 (2015).
- [12] S. Suchalkin, G. Belenky, and M. A. Belkin, "Rapidly tunable quantum cascade lasers," *IEEE J. Sel. Top. Quant.* 21, 1200509 (2015).
- [13] L. Nöhle, L. Hildebrandt, M. Kamp, and S. Höfling, "Interband cascade lasers: ICLs open opportunities for mid-IR sensing" *Laser Focus World* 49, 70-70 (May 2013)
- [14] I. Vurgaftman, W.W. Bewley, C.L. Canedy, S. K. Chul, K. Mijin, C. D. Merritt, J. Abell, and J. R. Meyer, "Interband cascade lasers with low threshold power and high output powers," *IEEE J. Sel. Top. Quant.* 19, 1200210 (2013).
- [15] A. Bauer, F. Langer, M. Dallner, M. Kamp, M. Motyka, G. Sek, K. Ryczko, J. Misiewicz, S. Höfling, and A. Forchel "Emission wavelength tuning of interband cascade lasers in the 3-4 μ m spectral range," *Appl. Phys. Lett.* 95, 251103 (2009).
- [16] Y. Cao, N. Sanchez, Wenzhe Jiang, R. J. Griffin, F. Xie, L. C. Hughes, C. Zah, and F. K. Tittel, "Simultaneous atmospheric nitrous oxide methane and water vapor detection with a single continuous wave quantum cascade laser," *Opt. Exp.* 23, 2121-2132 (2015).
- [17] D. R. Herriot, and H. J. Schulte, "Folded optical delay lines," *Appl. Opt.* 4, 883-889 (1965) .
- [18] J. U. White, "Long optical paths of large aperture," *J. Opt. Soc. America.* 32, 285-285 (1942).
- [19] G. Overton, "METROLOGY: new multipass gas cells beat conventional designs" *Laser Focus World* 49 (August 2013).
- [20] S. G. So, A. A. Sani, F. K. Tittel and G. Wysocki, "Ultra-compact multipass laser absorption spectroscopy platform for distributed sensor networks," *Conference on Lasers and Electro-Optics/International Quantum Electronics Conference, CMS2* (2009).
- [21] L. Dong, Y. Yu, C. Li, S. So, F. K. Tittel, "ppb-level formaldehyde detection using a CW room-temperature interband cascade laser and a miniature dense pattern multipass cell," *Opt. Express* 23, 19821-19830 (2015).